Inorganic Chemistry

Article

pubs.acs.org/IC

Layered Metal(IV) Phosphonates with Rigid Pendant Groups: New Synthetic Approaches to Nanosized Zirconium Phosphate Phenylphosphonates

Monica Pica,*[,†] Anna Donnadio,[†] Roberto D'Amato,[†] Donatella Capitani,[‡] Marco Taddei,[†] and Mario Casciola[†]

[†]Department of Chemistry, Perugia University, Via Elce di Sotto 8, 06123 Perugia, Italy

[‡]Istituto di Metodologie Chimiche, Laboratorio di Risonanza Magnetica "Annalaura Segre", CNR, Via Salaria km 29.300, 00016 Monterotondo Scalo (RM), Italy

ABSTRACT: Single phase mixed zirconium phosphate phenylphosphonates, $ZrP(PP)_x$, were prepared by two different synthetic approaches: reaction of gels of nanosized α-zirconium phosphate in propanol with solutions of phenylphosphonic acid (H_2PP), leading to the topotactic exchange of monohydrogen phosphate groups with phenylphosphonate groups, and precipitation from propanol solutions of H_2PP, phosphoric acid, and zirconyl propionate. In both cases, propanol intercalated compounds were obtained. The x values of the $ZrP(PP)_x$ materials prepared by topotactic anion exchange ranged from 0.37 to 0.56 for (H_2PP/Zr) molar ratios in the range 0.52−4.16 and [H_2PP] = 0.1 M, while a maximum x value of 0.73 was only reached at 60 °C, with (H_2PP/Zr) = 4.16 and [H_2PP] = 0.31 M. Direct precipitation of $ZrP(PP)_x$ provided samples with $0.13 \leq x \leq 1.54$, for H_2PP molar fractions in the range 0.05−0.5 and (P/Zr) molar ratio = 6. At 90% relative humidity, the (H_2O/Zr) molar ratio for the precipitated $ZrP(PP)_x$ powder samples increased in the range 1.3−3.0 with increasing x and resulted in being higher than that of nanosized ZrP (0.8). The analysis of the X-ray diffraction patterns of the gel and powder samples, together with the hydration data of the powder samples, suggested a structural model in which the random distribution of the phosphate and phenylphosphonate groups creates cavities which can accommodate propanol molecules in the gel samples and water molecules in the hydrated powder samples.

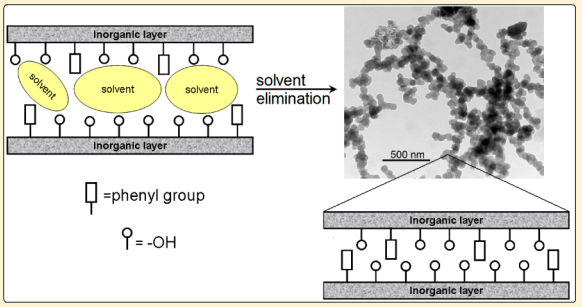

1. INTRODUCTION

The chemistry of layered metal(IV) phosphonates can be considered to have begun in 1978 when the first zirconium phosphonates with a layer structure of the α-type were synthesized.[1] Since then, these compounds were the object of intense research activity due to the possibility of their application in many fields, including use as polymer nanofillers,[2] catalysts,[3] and proton conductors.[4]

Zirconium phosphonates of the α-type are represented by the formula $Zr(O_3PR)_2$, or more in general $Zr(O_3PR)_{2-x}(O_3PR')_x$, where R and R′ are organic groups bonded to the phosphorus atom. The structure of the α-layers consists of a plane of Zr atoms where each Zr atom is coordinated to the oxygens of six phosphonates, while the oxygens of each phosphonate are bonded to three Zr atoms.[5] This kind of structure can be seen as obtained from that of α-zirconium phosphate ($Zr(O_3POH)_2 \cdot H_2O$, hereafter ZrP) by replacement of OH groups with organic groups.

The recent advances in the chemistry of layered zirconium phosphates and phosphonates led to the development of a new approach to the synthesis of α-type zirconium alkylphosphonates based on the reaction of gels of ZrP nanocrystals in propanol with alkylphosphonic acids,[6,7] consisting of the topotactic exchange of monohydrogen phosphate groups with alkylphosphonate groups. This quick and mild procedure allowed the phosphate groups of nanosized ZrP to partially be replaced with alkylphosphonate groups, obtaining, for the first time, single-phase mixed zirconium phosphate alkylphosphonates, with the alkyl chains randomly distributed on the α-type layers. The arrangement of groups with different size on the layers created "porous pathways" which turned out to be useful for the preparation of polymer composites, since they facilitate the diffusion of the polymer chains into the interlayer galleries of the inorganic filler.

Looking for new polymer fillers, it seemed of interest to extend the approach based on the topotactic anion exchange reaction of nanosized ZrP gels to the synthesis of other inorgano−organic layered compounds, such as zirconium phenylphosphonates. As well as being used as fillers in polymer composites,[8] zirconium phenylphosphonates are employed also as heterogeneous catalysts in oxidative reactions.[9]

The present paper reports the preparation of layered zirconium phosphate phenylphosphonates, with variable

Received: November 20, 2013
Published: January 28, 2014

   dx.doi.org/10.1021/ic402884g | *Inorg. Chem.* 2014, 53, 2222−2229

concentration of phenyl groups, according to two different synthetic strategies: topotactic anion exchange reaction of nanosized ZrP gels in propanol with phenylphosphonic acid solutions and direct precipitation according to the same "gel method"[6] employed for the synthesis of the nanosized ZrP gel in propanol. The material characterization, carried out by X-ray diffraction analysis, ^{31}P MAS NMR, and thermogravimetric analysis, allowed the two approaches to be compared and their application potentials to be evaluated.

2. EXPERIMENTAL SECTION

2.1. Chemicals. Zirconyl propionate ($ZrO_{1.27}(C_2H_5COO)_{1.46}$, MW = 218 Da) was supplied by MEL Chemicals, England. Phenylphosphonic acid ($C_6H_5PO_3H_2$, hereafter indicated as H_2PP) and all other reagents were supplied by Aldrich.

2.2. Synthesis of the Zirconium Phenylphosphonates by Topotactic Anion Exchange Reaction. Zirconium phenylphosphonates were synthesized by topotactic exchange reaction carried out on gels of nanosized ZrP in propanol, which were prepared according to ref 6. Specifically, 3.3 mmol of zirconyl propionate was dissolved in 10 mL of propanol. Concentrated phosphoric acid (14.8 M) was added, at room temperature under stirring, to the above solution so that the H_3PO_4/Zr molar ratio was 6. The clear solution obtained just after mixing turned into a semitransparent gel in a few minutes. The gel, after washing with propanol, contained about 8 wt % ZrP.

Phenylphosphonic acid was dissolved in propanol and a suitable amount of the H_2PP solution was added to the ZrP gel in propanol, so that the (H_2PP/Zr) molar ratio (hereafter R) was 0.52, 1.04, 2.08, and 4.16 with [H_2PP] = 0.1 M and R = 4.16 with [H_2PP] = 0.31 M. The mixtures were kept under stirring for 3 days at 25 or 60 °C; then, they were centrifuged, obtaining gelatinous precipitates, which were washed three times with propanol and dried in an oven at 60 °C. The resulting solids were washed in 10^{-3} M HCl, dried in an oven at 90 °C, and conditioned at 53% relative humidity.

2.3. Synthesis of the Zirconium Phenylphosphonates by Direct Precipitation. Concentrated phosphoric acid was added to a solution of phenylphosphonic acid in propanol, so that the H_2PP molar fraction was 0.050, 0.125, 0.250, 0.375, and 0.500. A suitable amount of the above solution was added to a solution of zirconyl propionate in propanol, so that the overall phosphorus concentration was 1 M and the (P/Zr) molar ratio was 6. The mixtures were kept under stirring at 25 °C for 1 day; then, they were centrifuged, obtaining gelatinous precipitates, which were washed three times with propanol and dried in an oven at 60 °C. The resulting solids were washed in 10^{-3} M HCl, dried in an oven at 90 °C, and conditioned at 53% relative humidity.

All the zirconium phenylphosphonates, prepared by topotactic anion exchange reaction and direct precipitation, will be hereafter indicated as $ZrP(PP)_x$.

2.4. Techniques. X-ray diffraction patterns of gels and powders were collected with a Philips X'Pert PRO MPD diffractometer operating at 40 kV and 40 mA, with a step size of 0.0334° and step scan of 25 s, using Cu Kα radiation and an X'Celerator detector.

Thermogravimetric determinations were carried out by a NETZSCH STA 449 Jupiter thermal analyzer connected to a NETZSCH TASC 414/3 A controller at a heating rate of 10 °C/min, with an air flow of about 30 mL/min.

Liquid ^{31}P NMR analysis was carried out by a Bruker Advance DPX 400 MHz on solutions obtained by dissolving the solid samples (≈30 mg) in 3 M HF (≈2 mL). The shifts of the phosphoric and phosphonic acid signals, relative to 85% D_3PO_4 in D_2O, were +0.7 and +15 ppm, respectively.

Solid state ^{31}P MAS NMR spectra were performed at 161.97 MHz on a Bruker Advance 400 spectrometer. The powders were packed into 4 mm zirconia rotors and sealed with Kel-F caps. The spin rate was 8 kHz. The $\pi/2$ pulse width was 3.5 s, and the recycle delay was 140 s; 1200 scans were collected for each spectrum. Spectra of powdered samples were acquired using 2048 data points. All spectra were zero filled and Fourier transformed. The chemical shift was externally referred to H_3PO_4 85%. The deconvolution of ^{31}P MAS spectra was performed using the DM2006 program.[10] The Gaussian/Lorentzian model was selected. Each resonance was characterized by the amplitude, the resonance frequency in parts per million (ppm), and the width at half-height.

Transmission electron microscopy (TEM) analysis was carried out by a Philips 208 transmission electron microscope, operating at an accelerating voltage of 100 kV. Powders were rapidly diluted in ethanol and sonicated for a few minutes, then supported on copper grids (200 mesh) precoated with Formvar carbon films, and quickly dried.

The (P/Zr) molar ratio of all the $ZrP(PP)_x$ samples was determined by using an ICP Varian Liberty inductively coupled plasma-optical emission spectrometer (ICP-OES) with axial injection. A weighed amount of the samples was dissolved in 3 M HF (≈2 mL) and then diluted with water.

The water uptake tests were performed at room temperature, by equilibritating the powder samples at 90% relative humidity for 1 week. Then, the samples were dried at 100 °C overnight; the (H_2O/Zr) molar ratio was determined on the basis of the difference between the weight of the hydrated and anhydrous sample.

3. RESULTS AND DISCUSSION

3.1. Topotactic Anion Exchange Reaction. ZrP gels in propanol were put in contact with solutions of phenylphosphonic acid in propanol so that the (H_2PP/Zr) molar ratio (R) was 0.52, 1.04, 2.08, and 4.16.

Figure 1 shows a representative ^{31}P MAS NMR spectrum of a $ZrP(PP)_x$ sample, synthesized at 25 °C for R = 2.08 and [H_2PP] = 0.1 M.

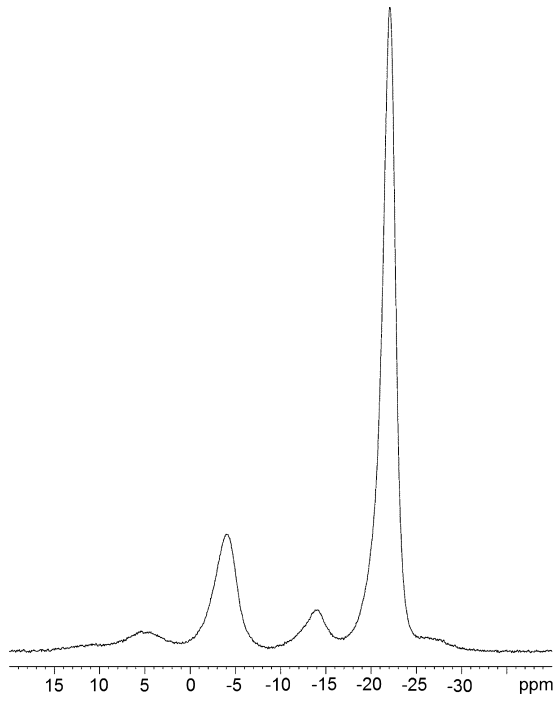

Figure 1. ^{31}P MAS NMR spectrum of a $ZrP(PP)_x$ sample, synthesized at 25 °C for R = 2.08 and [H_2PP] = 0.1 M.

According to the literature, the two main signals at −22.1 and −3.9 ppm are assigned to the phosphate and phenyl phosphonate groups, respectively, bonded through the oxygens to three Zr(IV) atoms:[11] this is the typical Zr(IV) coordination in M(IV) phosphates and phosphonates with layer structure of the α-type. Moreover, the two weaker signals at −13.8 and +5.0 ppm are attributed to the phosphate and phenylphosphonate

dx.doi.org/10.1021/ic402884g | Inorg. Chem. 2014, 53, 2222−2229

groups, respectively, connected to two Zr(IV) atoms. The very weak signal at 10.6 ppm can be assigned to phosphonate groups bonded to one zirconium atom.

From the peak deconvolution, it has been found that the percentage of the double-connected phosphate and phosphonate groups was less than 10% of the total groups: similar results were obtained for the zirconium phosphate alkylphosphonates prepared by topotactic anion exchange reaction.[7] Taking into account that the (P/Zr) molar ratio, determined by ICP analysis, was around 1.95 for all materials, the following general formula for $ZP(PP)_x$ can be written:

$$Zr(OH)_{0.1+(x'+y')}[O_2P(OH)C_6H_5]_{x'}(O_3PC_6H_5)_{x''}[O_2P(OH)_2]_{y'}(O_3POH)_{y''}$$

Setting $x' + x'' = x$, $y' + y'' = y$, and $x + y = 1.95$, the formula can be simplified as follows:

$$Zr(OH)_{0.1}(O_3PC_6H_5)_x(O_3POH)_{1.95-x}\cdot(x' + y')H_2O$$

The phosphate to phosphonate molar ratio (x/y) was determined by ^{31}P liquid and MAS NMR analysis, and the average x values were reported in Table 1.

Table 1. Chemical Composition and Interlayer Distances, Determined by X-ray Analysis, of $ZrP(PP)_x$ Powder Samples Obtained by Topotactic Anion Exchange Reaction

T (°C)	$[H_2PP]$ (M)	R	x	interlayer distance (Å)
25	0.10	0.52	0.37 ± 0.02	11.2 ± 0.5
25	0.10	1.04	0.61 ± 0.02	11.7 ± 0.7
25	0.10	2.08	0.56 ± 0.05	11.7 ± 1.0
25	0.10	4.16	0.65 ± 0.03	11.9 ± 0.7
25	0.31	4.16	0.54 ± 0.03	11.3 ± 0.6
60	0.31	4.16	0.73 ± 0.04	12.3 ± 1.1

It can be observed that, at 25 °C and for $R \geq 1.04$, the x values are essentially independent of R and of the H_2PP concentration lying in the range 0.59 ± 0.06. Surprisingly, even by increasing the reaction temperature to 60 °C, the x value keeps below 1, with less than half of the phosphate groups of ZrP exchanged with phenylphosphonate groups. A similar result was obtained also for the topotactic exchange reaction of nanosized ZrP with alkylphosphonic acids.[7] As previously reported, one should consider that the reactions involving solids generally begin in the external part of the crystals and then proceed toward the internal part. Since the pristine material consists of propanol intercalated ZrP nanosheets, initially the phosphonic acid can easily diffuse within the layers and react. As the reaction proceeds, the reacted phase will result enriched in phosphonate groups and, especially at high R values, the protruding and rigid phenylphosphonate groups are expected to hamper the diffusion of additional phosphonic acid molecules within the interlayer space and their reaction with Zr(IV).

The thermal stability of $ZrP(PP)_x$ was evaluated by thermogravimetric (TG) analysis under an oxygen rich atmosphere. Figure 2 shows a typical weight loss curve of the $ZP(PP)_{0.56}$ powder sample.

Two steps were observed: the first one, centered around 100 °C, arises from the loss of adsorbed and/or intercalated water. The second step, centered around 500 °C, can be mainly attributed to the decomposition of the organic moieties and to the loss of water arising from the condensation of residual

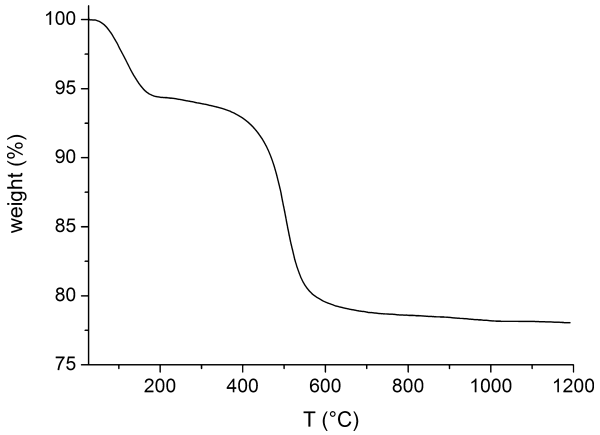

Figure 2. Thermogravimetric curve of $ZrP(PP)_{0.56}$, obtained by topotactic exchange reaction.

HPO_4 groups with the formation of zirconium pyrophosphate. On the basis of these considerations, the following reaction scheme can be considered:

step 1:

$$Zr(O_3PC_6H_5)_x(O_3POH)_{1.95-x}(OH)_{0.1}\cdot nH_2O \xrightarrow{-nH_2O} Zr(O_3PC_6H_5)_x(O_3POH)_{1.95-x}(OH)_{0.1}$$

step 2:

$$Zr(O_3PC_6H_5)_x(O_3POH)_{1.95-x}(OH)_{0.1} \xrightarrow{O_2} 0.975ZrP_2O_7 + 6xCO_2 + 0.025ZrO_2 + (2x + 1.025)H_2O$$

It was possible to calculate the composition of the materials from the second weight loss: as an example, the x value, calculated for the $ZrP(PP)_x$ sample obtained for $R = 2.08$, was 0.60, in good agreement with that found from ^{31}P NMR analysis. In all cases, the difference between the x values calculated from NMR analysis and those calculated from TG analysis was ≤10%. This difference can be partially attributed to the fact that the determination of the chemical composition, on the basis of the thermogravimetric data, is affected to some extent by the uncertainty in the selection of the point, on the thermogravimetric curve, where step 1 ends and step 2 starts.

Parts A and B of Figure 3 show the TEM images of $ZP(PP)_{0.65}$ and the pristine α-ZrP powder samples, respectively. It can be observed that the zirconium phosphonate sample is made of aggregates consisting of particles with a size of some tens of nanometers. A similar particle size was found for powders of zirconium phosphate alkylphosphonates prepared by topotactic anion exchange from α-ZrP gels in propanol[7] and for the α-ZrP nanocrystals of these gels.[6] However, differently from the organically modified materials, the nanocrystals of the α-ZrP gel fuse together and increase their size after solvent elimination, so that the resulting powder consists of layered particles with planar size in the range 50−300 nm. It might therefore be inferred that the presence of the organic groups, anchored to the α-layers, hinders to some extent the expected particle growth.

Figures 4 and 5 report the X-ray diffraction patterns of the $ZrP(PP)_x$ gel and powder samples, respectively, obtained for different R values. As observed for the ZrP gel in propanol

dx.doi.org/10.1021/ic402884g | Inorg. Chem. 2014, 53, 2222−2229

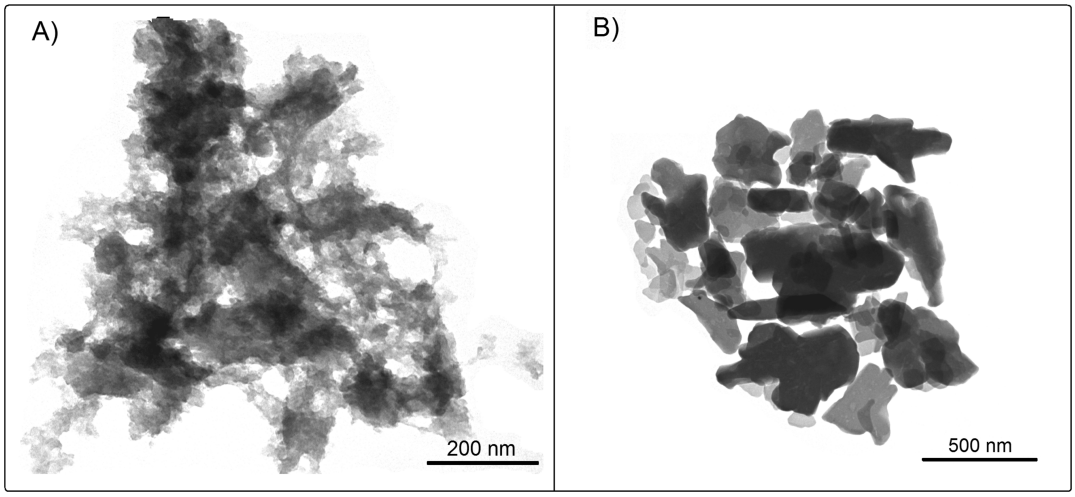

Figure 3. TEM images of $ZrP(PP)_{0.65}$ (A) and the pristine ZrP (B) powder samples.

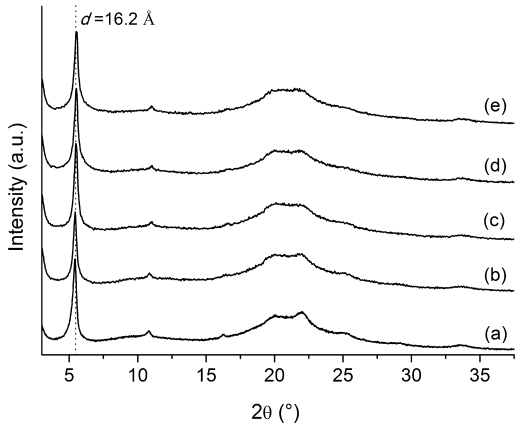

Figure 4. X-ray diffraction patterns of gels in propanol for pristine ZrP (a) and $ZrP(PP)_x$ samples obtained at 25 °C by topotactic exchange reaction with x = 0.37 (b), 0.61 (c), 0.56 (d), and 0.65 (e).

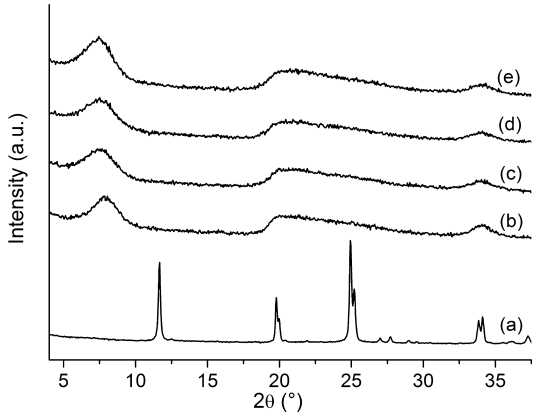

Figure 5. X-ray diffraction patterns of powder samples obtained by drying the corresponding gels: pristine ZrP (a) and $ZrP(PP)_x$ samples obtained at 25 °C by topotactic exchange reaction with x = 0.37 (b), 0.61 (c), 0.56 (d), and 0.65 (e).

(pattern a), the X-ray patterns of the $ZrP(PP)_x$ gel samples show the presence of a well-defined peak at 5.5° 2θ, corresponding to an interlayer distance of 16.2 Å, which is the same as that of ZrP intercalated with propanol, containing 2 mol of alcohol/mol of ZrP.[6]

When the gels are dried, the reflection at 33.8° 2θ (d-spacing = 2.65 Å), typical of the Zr−Zr separation in the α-type layer, becomes more evident. The presence of this reflection together with the ^{31}P MAS NMR data proves that the reaction of nanosized ZrP with phenylphosphonic acid is a topotactic anion exchange reaction, which does not alter the inorganic framework of the α-layer.

Figure 5 also shows that the powder samples are, on the whole, less crystalline than the unmodified nanosized ZrP; after heating the gel samples, the first reflection becomes broader and shifts toward lower d-values. The low degree of crystallinity of the $ZrP(PP)_x$ samples does not allow an accurate structural evaluation. However, as shown in Table 1, the interlayer distances of all powder samples lie between those of the pure phenylphosphonate $Zr(PP)_2$ (d = 14.7 Å)[11b] and phosphate phases (d = 7.6 Å):[5] this fact, as well as the absence of ZrP reflections other than that at 33.8° 2θ, indicates that the topotactic exchange reaction leads to the formation of single-phase mixed zirconium phosphate phenylphosphonates with the phenyl rings anchored to the α-layers and randomly distributed among the unreacted monohydrogen phosphate groups.

It should be pointed out that the $ZrP(PP)_x$ compounds synthesized in this work are the first example of single-phase mixed zirconium phosphate phenylphosphonates obtained by a topotactic anion exchange reaction, since in a previous work by Hix et al. the topotactic exchange replacement of monohydrogen phosphate groups with phenylphosphonate groups on semicrystalline ZrP led to mixtures of pure phases of ZrP and α-zirconium phenylphosphonate with constant composition.[12]

3.2. Direct Precipitation. The approach based on the topotactic anion exchange reaction did not allow the material composition to be controlled, which turned out to be independent of R for $R \geq 1.0$. Therefore, in order to investigate the possibility to prepare single-phase mixed compounds with a variable concentration of phenylphosphonate groups, a second approach has been considered, consisting of the direct precipitation of $ZrP(PP)_x$ compounds from propanol solutions of zirconyl propionate, H_3PO_4 and H_2PP, according to the same "gel method" employed for the synthesis of the nanosized ZrP in propanol.[6] It was observed that, for low values of H_2PP molar fraction in the mother solution, semitransparent gels, similar to that of nanosized ZrP, were obtained after 1 day of

dx.doi.org/10.1021/ic402884g | Inorg. Chem. 2014, 53, 2222−2229

Table 2. Chemical Composition and Interlayer Distances of $ZrP(PP)_x$ Samples Obtained by Direct Precipitation

total phosphorus in solution (mol/L)	H_2PP molar fraction in solution	P_{tot}/Zr molar ratio in solution	x	interlayer distance (Å)	
				gel	powder
1.0	0.050	6	0.13 ± 0.01	16.2 ± 0.1	11.0 ± 0.6; 7.6 ± 0.2
1.0	0.125	6	0.43 ± 0.02	16.2 ± 0.1	11.3 ± 0.3
1.0	0.250	6	0.82 ± 0.03	15.7 ± 0.2	12.7 ± 0.3
1.0	0.375	6	1.30 ± 0.02	15.4 ± 0.2	14.5 ± 0.2
1.0	0.500	6	1.54 ± 0.02	15.0 ± 0.2	14.5 ± 0.3

reaction time; with increasing amount of H_2PP in the mother solution, the just formed gel turned into a white precipitate after 1 day. The conditions for the direct precipitation of the $ZrP(PP)_x$ compounds and their composition are reported in Table 2. In all cases, the overall (P/Zr) molar ratio in the solids, determined by ICP analysis, was around 1.95.

The synthesis of $ZrP(PP)_x$ by direct precipitation allowed compounds with x ranging from 0.13 to 1.54 to be obtained.

In order to better highlight the relationship between the initial amount of phosphonic acid in solution and that found in the final product, the PP molar fraction in the solids, having composition $Zr(O_3PC_6H_5)_x(O_3POH)_{1.95-x}(OH)_{0.1}$, was calculated according to the formula:

$$(\text{PP molar fraction})_{\text{solid}} = \frac{x}{1.95}$$

and plotted against the H_2PP molar fraction in the mother solutions. The experimental data were reported in Figure 6,

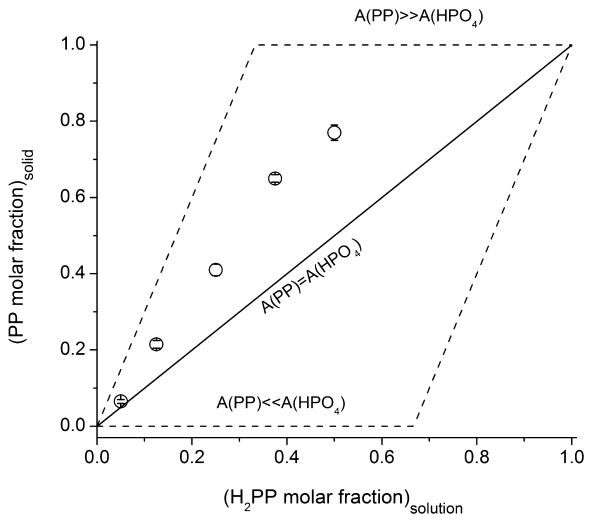

Figure 6. Composition of $ZrP(PP)_x$ as a function of the initial composition of the mother solution for a P_{tot}/Zr(IV) molar ratio of 6. $A(HPO_4)$ and $A(PP)$ are the Zr(IV) affinities for HPO_4 and PP, respectively. Dashed and solid lines represent the expected composition for the indicated affinity relations.

together with those calculated on the basis of different affinities of Zr(IV) for the phenylphosphonate and phosphate anions. The upper dashed line was calculated by assuming that the Zr(IV) affinity for the phenylphosphonate anion ($A(SPP)$) is much higher than that for monohydrogen phosphate ($A(HPO_4)$), so that Zr(IV) reacts with all available H_2PP, when $H_2PP/Zr(IV) \leq 2$, or forms $Zr(PP)_2$ if $H_2PP/Zr(IV) > 2$. Similarly, the lower dashed curve was obtained for $A(HPO_4) \gg A(PP)$, while the solid line was calculated for $A(HPO_4) = A(PP)$. It can be observed that the experimental data lie between the upper dashed line and the solid line, indicating that the phenylphosphonate groups have a higher affinity toward Zr(IV) than the monohydrogen phosphate groups, especially for the highest values of H_2PP molar fraction. This result is quite surprising, since a completely opposite behavior was found for the precipitation of zirconium phosphate sulfophenylphosphonates from aqueous solutions of ZrF_6^{2-}, H_3PO_4, and meta-sulfophenylphosphonic acid (H_2SPP).[13] Among other factors, the different solvation energies of H_2PP and H_2SPP in propanol and water, respectively, could play an important role in the precipitation of the corresponding zirconium phosphonates. It is reasonable to suppose that, due to the presence of the acid sulfonic group, H_2SPP in water is much more solvated with respect to H_2PP in propanol: the stronger solvent interaction should make H_2SPP less reactive than H_2PP toward Zr(IV). Moreover, one should also consider that the $-SO_3H$ group in the meta-position on the aryl ring in H_2SPP could reduce the electron density of the $-PO_3H_2$ group and, consequently, its reactivity toward Zr(IV).

It can be oserved that the composition data of the materials obtained by direct precipitation, reported in Table 2, provide further support to the idea that the reaction between nanosized α-ZrP and an H_2PP solution is a topotactic anion exchange process. In fact, if the supposed topotactic exchange reaction were instead a dissolution−reprecipitation process, the phosphonate molar fraction in solution, for an initial (H_2PP/Zr) molar ratio of 4.16, would be never lower than 0.5, since the maximum amount of phosphate species that the solid can release to the solution is half the initial phosphonate amount. Under these conditions, according to the data of Table 2, the precipitation would lead to the formation of solids with $x > 1.5$, much richer in phosphonate than the solids that were actually obtained.

The thermal behavior of the materials obtained by direct precipitation was also similar to that reported for the exchanged materials, and Figure 7 shows a typical weight loss curve of the $ZrP(PP)_x$ samples obtained by direct precipitation.

The TEM image of a $ZrP(PP)_{1.54}$ sample is reported in Figure 8. It consists of flat particles of tens of nanometers, having very regular size and shape, and smaller than that of nanosized ZrP shown in Figure 3.

Figures 9 and 10 show the X-ray diffraction patterns of the $ZrP(PP)_x$ gels and powders, respectively, obtained for different x values. The diffraction patterns of the gels resemble that of the nanosized ZrP gel in propanol, with a strong reflection at low 2θ values that shifts to higher 2θ values with increasing x.

After the gels are dried, the reflection at 33.8° 2θ becomes more evident in all the powder patterns, while the first reflection becomes wider and moves toward lower 2θ values with increasing PP content. It is also noteworthy that the reflections of ZrP (at 11.63, 4.48, and 3.56° 2θ) are observed only in the pattern of the $ZrP(PP)_{0.13}$ powder sample,

dx.doi.org/10.1021/ic402884g | Inorg. Chem. 2014, 53, 2222−2229

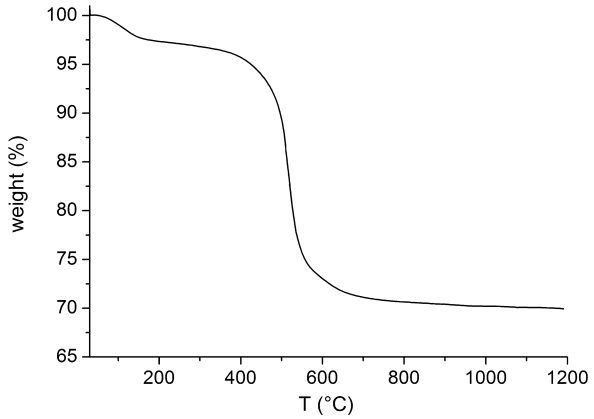

Figure 7. Thermogravimetric curve of $ZrP(PP)_{1.30}$, obtained by direct precipitation.

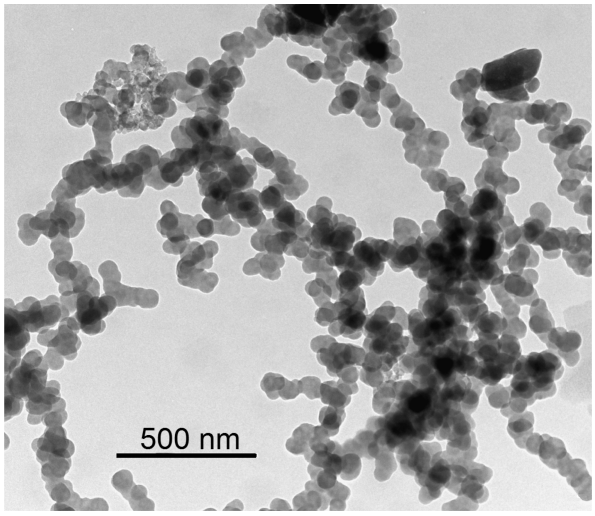

Figure 8. TEM image of the $ZrP(PP)_{1.54}$ powder sample.

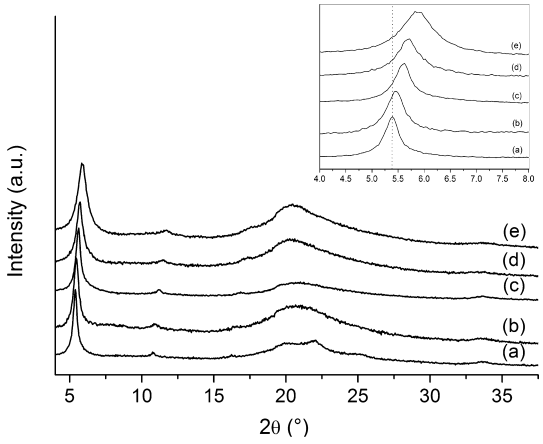

Figure 9. X-ray diffraction patterns of $ZrP(PP)_x$ gels obtained by direct precipitation with x = 0.13 (a), 0.43 (b), 0.82 (c), 1.30 (d), and 1.54 (e).

suggesting that the formation of ZrP is promoted at very low H_2PP content in the reaction solution.

Recalling that the reflection at 33.8° 2θ is associated with the Zr−Zr separation in the α-type layer of Zr(IV) phosphate and phosphonate,[5] the presence of this reflection in all the X-ray patterns of the $ZrP(PP)_x$ samples indicates that the direct

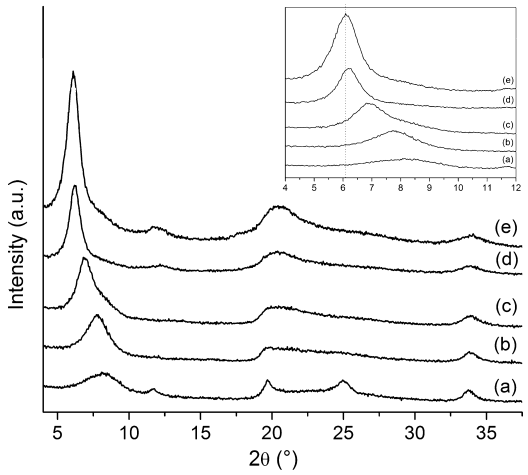

Figure 10. X-ray diffraction patterns of the $ZrP(PP)_x$ of powder samples obtained by direct precipitation, by drying the corresponding gels: x = 0.13 (a), 0.43 (b), 0.82 (c), 1.30 (d), and 1.54 (e).

precipitation leads to the formation of layered compounds of the α-type. Additional structural information can be obtained by plotting the interlayer distances, of both gels and powders, as a function of the solid composition (Figure 11).

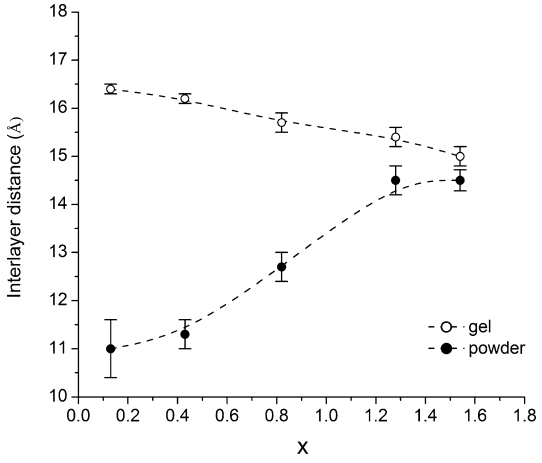

Figure 11. Interlayer distances of $ZrP(PP)_x$ gel and powder samples, obtained by direct precipitation, as a function of x.

On the basis of the data reported in Figure 11, several considerations can be done:

(a) The interlayer distance of the gel samples slightly decreases with increasing x, ranging from that of pure propanol intercalated ZrP (16.2 Å) to that of pure $Zr(PP)_2$ (14.7 Å).

(b) The interlayer distance of the powder samples gradually increases with increasing x, being higher than that of ZrP and lower than that of pure $Zr(PP)_2$; as a consequence, the interlayer distance of the powder samples is significantly lower than that of the corresponding gel samples at low PP contents, while they become nearly coincident for $x \approx 1.6$.

(c) The fact that the interlayer distance of the $ZrP(PP)_x$ compounds never exceeds 14.7 Å allows one to exclude the formation of staged compounds, having an interlayer distance between 22.5 and 25.4 Å, that according to

dx.doi.org/10.1021/ic402884g | Inorg. Chem. 2014, 53, 2222−2229

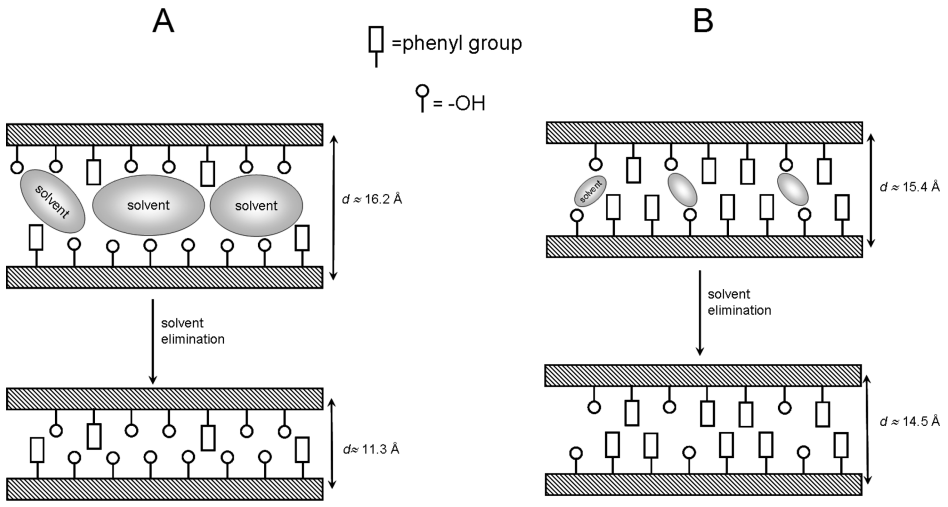

Figure 12. Schematic model showing the possible arrangement of phosphate and phenylphosphonate groups in $ZrP(PP)_x$ for low PP contents (A) and high PP contents (B) and the resulting interlayer changes due to the solvent deintercalation from the gel samples.

Clearfield et al. are generally obtained when the phosphate to phosphonate ratio is ≥1.[11b]

(d) The formation of ZrP for the lowest H_2PP content in the mother solution did not allow the exact composition of the mixed phase having an interlayer distance of 11.0 Å to be known; however, since the interlayer distance of the powder samples increases with increasing PP content, it is reasonable to suppose that the x value of the solid, obtained for an H_2PP molar fraction of 0.05 in the mother solution, is lower than that of the solid obtained for an H_2PP molar fraction of 0.125, that is $x < 0.43$.

Taking into account the above observations and the fact that, except for $x = 0.13$, the X-ray patterns of the $ZrP(PP)_x$ samples do not show ZrP reflections other than that at 33.8 2θ, it is concluded that all the $ZrP(PP)_x$ compounds with $x \geq 0.43$ can be considered as single-phase mixed zirconium phosphate phenylphosphonates. As in the case of the materials obtained by topotactic anion exchange, phosphate and phenylphosphonate groups are supposed to be randomly distributed on the surface of the α-layers according to the schematic model depicted in Figure 12.

For low x values, solvent molecules can be accommodated in the interlayer region in a fashion similar to that of the propanol intercalated ZrP. When the solvent is removed, the interlayer distance significantly decreases with formation of cavities due to the presence of the phenylphosphonates groups dispersed on the surface of the $ZrP(PP)_x$ α-layers. With increasing fraction of phenylphosphonate groups, the cavities become smaller and a lower number of solvent molecules are intercalated, so that the interlayer distance of the $ZrP(PP)_x$ gel samples approaches that of the powder samples.

The structural model of Figure 12 suggests that the cavities generated by the random distribution of the phenyl groups might make the interlayer region more accessible to the water molecules than in ZrP. On the other hand, the phenyl groups are expected to reduce the hydrophilic character of the α-layers. It was therefore of interest to determine the hydration of $ZrP(PP)_x$ powder samples, equilibrated at 90% relative humidity at room temperature. Figure 13 shows the hydration of the $ZrP(PP)_x$ samples, expressed as water molecules per Zr atom, as a function of x; the (H_2O/Zr) molar ratio of nanosized ZrP was also reported for comparison. It can be observed that,

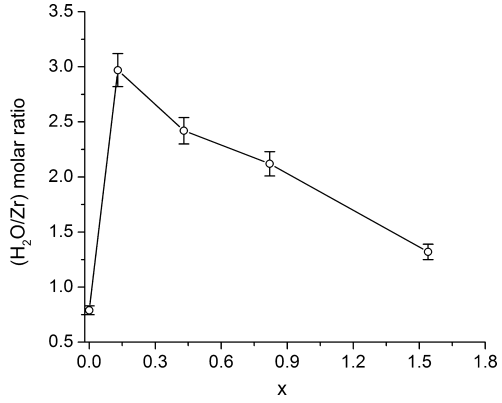

Figure 13. Water uptake, at room temperature and 90% relative humidity, for $ZrP(PP)_x$ powder samples, obtained by direct precipitation, as a function of x. The value for a PP molar fraction of 0 refers to nanosized ZrP.

as expected, the water uptake decreases with increasing x and that all the $ZrP(PP)_x$ samples exhibit a higher water content with respect to nanosized ZrP.

The water content of the sample with the lowest PP content is nearly 4 times higher than that of nanosized ZrP. It is also noteworthy that, even at 53% relative humidity, the water content of $ZrP(PP)_{0.43}$ ($H_2O/Zr = 1.6$) is larger than that of ZrP at 90% relative humidity. These findings show unambiguously that, in spite of their hydrophobic character, the presence of the phenyl groups anchored to the α-layers favors the hydration of the interlayer region.

Further structural information was obtained by ^{31}P MAS NMR. In all cases, the spectra of the powder samples exhibit the same resonances observed for the samples obtained by topotactic anion exchange. As an example, the spectra of $ZrP(PP)_{0.82}$ and $ZrP(PP)_{1.54}$ are reported in Figure 14. The evolution of the areas of the deconvoluted peaks shows that the amount of double-connected phosphate and phosphonate groups increases with x. In particular, while the percentage of double connected phosphate groups is in all cases less than 5% of the overall phosphorus content, the percentage of phosphonate groups with low connectivity is less than 17% for $x \leq 1.30$ but reaches 35% for $x = 1.54$.

dx.doi.org/10.1021/ic402884g | Inorg. Chem. 2014, 53, 2222−2229

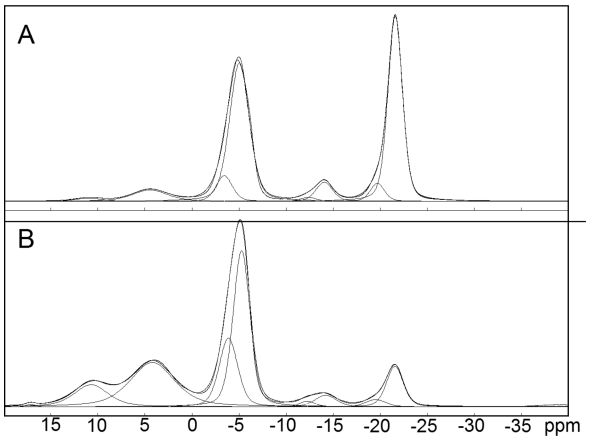

Figure 14. ^{31}P MAS NMR spectra of the $ZrP(PP)_{0.82}$ (A) and $ZrP(PP)_{1.54}$ (B) samples; the deconvoluted peaks are also shown.

Taking into account that the X-ray data are characteristic of α-layered crystalline phases (where phosphate and phosphonate groups are triply-connected to Zr(IV) atoms) while the NMR data reveal also the presence of phosphate and phosphonate groups with lower connectivity, it can be reasonably suggested that the increase in x leads to the formation of increasingly defective α-layers and even to an amorphous phase for the highest x values. As a consequence, the structural model depicted in Figure 12 appears more representative for the compounds with the lowest x values. In our opinion, these are the most interesting materials, since they are characterized by the largest accessible interlayer space as proved by the higher water uptake of the powder samples with respect to nanosized ZrP.

CONCLUSIONS

Layered zirconium phosphate phenylphosphonates, with phosphate and phosphonate groups "interdispersed" on the surface of the layers, were prepared by two different approaches: topotactic anion exchange reaction of nanosized ZrP with phenylphosphonic acid and direct precipitation in propanol by using the "gel method". In both cases, propanol intercalated single phase compounds were obtained, consisting of flat particles with a planar size of tens of nanometers.

The composition of the materials obtained by topotactic anion exchange reaction turned out to be almost invariant within a wide range of R values and weakly dependent on temperature. On the other hand, a better control of the phenylphosphonate content was achieved by the direct precipitation approach, just varying the H_2PP/H_3PO_4 molar ratio in the mother solution containing Zr(IV); it was observed that the fraction of PP groups in the solids was higher than that in the mother solution, indicating that the Zr(IV) affinity for the phenylphosphonate anion is higher than that for monohydrogen phosphate. The random distribution of small phosphate groups and large phenylphosphonate groups on the layer surface suggested the formation of cavities in the interlayer region, where water molecules can be accommodated. Accordingly, under the same relative humidity, $ZrP(PP)_x$ samples turned out to be more hydrated than ZrP. These materials are expected to be suitable fillers for the preparation of polymer nanocomposites based on both neutral polymers, such as polystyrene, and ionomers, such as polyetherketones.

AUTHOR INFORMATION

Corresponding Author

*E-mail: monica.pica@unipg.it. Phone: +39 075 585 5564. Fax: +39 075 585 5566.

Notes

The authors declare no competing financial interest.

REFERENCES

(1) Alberti, G.; Costantino, U.; Allulli, S.; Tomassini, N. *J. Inorg. Nucl. Chem.* **1978**, *40*, 1113.

(2) (a) Alberti, G.; Casciola, M.; Pica, M.; Di Cesare, G. *Ann. N. Y. Acad. Sci.* **2003**, *984*, 208−225. (b) Alberti, G.; Casciola, M.; D'Alessandro, E.; Pica, M. *J. Mater. Chem.* **2004**, *14*, 1910−1914T. (c) Alberti, G.; Casciola, M.; Pica, M.; Tarpanelli, T.; Sganappa, M. *Fuel Cells* **2005**, *5*, 366−374. (d) Casciola, M.; Capitani, D.; Donnadio, A.; Diosono, V.; Piaggio, P.; Pica, M. *J. Mater. Chem.* **2008**, *18*, 4291−4296. (e) Casciola, M.; Capitani, D.; Donnadio, A.; Frittella, V.; Pica, M.; Sganappa, M. *Fuel Cells* **2009**, *4*, 381−386. (f) Sun, L.; Liu, J.; Kirumakki, S. R.; Schwerdtfeger, E. D.; Howell, R. J.; Al-Bahily, K.; Miller, S. A.; Clearfield, A.; Suef, H.-J. *Chem. Mater.* **2009**, *21*, 1154−1161. (g) Donnadio, A.; Pica, M.; Taddei, M.; Vivani, R. *J. Mater. Chem.* **2012**, *22*, 5098.

(3) (a) Colón, J. L.; Thakur, D. S.; Yang, C.-Y.; Clearfield, A.; Martini, C. R. *J. Catal.* **1990**, *124*, 148−159. (b) Curini, M.; Rosati, O.; Costantino, U. *Curr. Org. Chem.* **2004**, *8*, 591−606. (c) Bellezza, F.; Cipiciani, A.; Costantino, U.; Nicolis, S. *Langmuir* **2004**, *20*, 5019−5025. (d) Ma, X.; Wang, Y.; Wang, W.; Cao, J. *Catal. Commun.* **2010**, *11*, 401−407. (e) Chen, T.; Ma, X.; Wang, X.; Wang, Q.; Zhou, J.; Tang, Q. *Dalton Trans.* **2011**, *40*, 3325.

(4) (a) Alberti, G.; Casciola, M.; Costantino, U.; Peraio, A.; Montoneri, E. *Solid State Ionics* **1992**, *50*, 315−322. (b) Alberti, G.; Casciola, M.; Palombari, R.; Peraio, A. *Solid State Ionics* **1992**, *58*, 339−344. (c) Alberti, G.; Boccali, L.; Casciola, M.; Massinelli, L.; Montoneri, E. *Solid State Ionics* **1996**, *84*, 97−10.

(5) *Comprehensive Supramolecular Chemistry, Two and Three-dimensional Inorganic Networks*; Alberti, G., Bein, T., Eds.; Pergamon, Elsevier Ltd. Press: Oxford, U.K., 1996; Vol. 7, Chapters 4−5.

(6) Pica, M.; Donnadio, A.; Capitani, D.; Vivani, R.; Troni, E.; Casciola, M. *Inorg. Chem.* **2011**, *50*, 11623−11630.

(7) Pica, M.; Donnadio, A.; Troni, E.; Capitani, D.; Casciola, M. *Inorg. Chem.* **2013**, *52*, 7680−7687.

(8) (a) Liu, C.; Zhu, L.; Wu, H.; Yang, Y. *J. Appl. Polym. Sci.* **2011**, *119*, 2334−2338. (b) Hill, M. L.; Einsla, B. R.; Kim, Y. S.; McGrath, J. E. *Prepr. Pap.—Am. Chem. Soc., Div. Fuel Chem.* **2004**, *49*, 584−585.

(9) (a) Rocha, G. M. S. R. O.; Domingues, R. M. A.; Simões, M. M. Q.; Silva, A. M. S. *Appl. Catal., A* **2009**, *353*, 236−242. (b) Rocha, G. M. S. R. O.; Santos, T. M.; Bispo, C. S. S. *Catal. Lett.* **2011**, *141*, 100−110. (c) Lanari, D.; Montanari, F.; Marmottini, F.; Piermatti, O.; Orrù, M.; Vaccaro, L. *J. Catal.* **2011**, *277*, 80−87.

(10) Massiot, D.; Fayon, F.; Capron, M.; King, I.; LeCalv, S.; Alonso, B.; Durand, J. O.; Bujoli, B.; Gan, Z.; Hoatson, G. *Magn. Reson. Chem.* **2002**, *40*, 70.

(11) (a) Clayden, N. *J. Chem. Soc., Dalton Trans.* **1987**, *8*, 1877. (b) Clearfield, A.; Wang, J. D.; Tian, Y.; Stein, E.; Bhardwaj, C. *J. Solid State Chem.* **1995**, *117*, 275−289.

(12) Hix, G. B.; Kitchin, S. J.; Harris, K. D. M. *J. Chem. Soc., Dalton Trans.* **1998**, 2315−2319.

(13) Alberti, G.; Casciola, M.; Donnadio, A.; Piaggio, P.; Pica, M.; Sisani, M. *Solid State Ionics* **2005**, *176*, 2893−2898.